

# QUANTIFICATION OF DAMAGE EVOLUTION IN MULTILAYERED HIGH TEMPERATURE COMPOSITES FROM ULTRASONIC MEASUREMENTS

A. D. Degtyar<sup>1</sup> and S. I. Rokhlin

The Ohio State University  
Nondestructive Evaluation Program  
1248 Arthur E. Adams Drive  
Columbus, Ohio 43221

## INTRODUCTION

New high temperature composite materials have potential to yield significant performance improvement and weight reduction in different components for aerospace applications (i.e. aircraft engines, airframe parts). For successful application of these materials in various environments their mechanical properties, life service capability and reliability must be known. The high cost of structures engineered from these materials makes experimental life determination very difficult. Thus the development of methodology for NDE of structures, combined with life prediction models using measured damage as input data, becomes very important.

The structural parts made from these materials are expected to operate at elevated temperatures under cyclic or static loading. The resulting thermal and mechanical stresses can significantly affect the performance of these materials by causing damage. The level of damage may vary for different constraints, geometries and loading histories in structures. Due to the inhomogeneous and anisotropic nature of these materials their damage mechanisms differ significantly from conventional monolithic materials. In addition to crack initiation and growth in the matrix material fatigue in composites results in fiber-matrix interface debonding and fiber breakage. For example for high cycle fatigue (low stress level) the common damage mechanism is cracks initiated at the fiber-matrix interface (mostly in reaction zone) [1, 2, 3, 4]. For low cycle fatigue typical damage mechanisms are interfacial debonding in the off-axis plies followed by matrix cracking [3].

To characterize fatigue damage evolution one can utilize ultrasonic bulk wave velocity measurements [5]. The concept of the previously described method and the method utilized in this study is following. Angular dependence of ultrasonic phase velocities is measured at different stages of fatigue life. The reduction of effective composite moduli is associated with fatigue-induced damage. The composite elastic moduli are determined from the velocity data using a nonlinear least squares inversion technique. Micromechanical analysis is utilized to relate changes in effective elastic

---

<sup>1</sup>is now with Thiokol Corporation Research & Development Lab.,  
P.O. Box 707, Brigham City, UT 84302-0707

moduli to damage characteristics of different layers. A similar strategy has been used by Baste and co-workers [6] for characterization of damage in ceramic matrix composites. In their work the main damage mechanism was assumed to be matrix microcracking. The damage was characterized by crack density and their orientation with respect to the loading direction.

In our previous study a partial debond model [5] has been utilized to predict effective composite moduli of SiC/Ti cross-ply composite. This method describes a specific damage state corresponding to approximately 50% of the fatigue life. In this paper we propose a model of damage evolution which is based on an application of a micromechanical analysis (Generalized Method of Cells (GMC)) developed by Aboudi [7, 8]. We utilize the GMC codes developed in NASA-Lewis Research Center [9]. First damage is modeled in unidirectional composites when fatigue direction is perpendicular to the fibers. Micromechanical damage parameters describing the debonding are introduced which characterize damage evolution in the initial stages of the fatigue life. GMC is used to determine the dependence of effective composite moduli on these damage parameters. The damage model for [90] laminate is extended to describe the damage in [0/90] cross-ply composite. The inversion is used to determine the damage parameters from the reduction of the effective composite moduli. This allows one to quantify fatigue damage in multilayered composites and thus to monitor damage initiation and development. The model developed is applied to monitor fatigue damage evolution in [0/90] SiC/Ti-15V-3Cr-3Al-3Sn metal matrix composite. The measured effective composite moduli are used to characterize the fatigue damage evolution. For detailed description of the experimental method and ultrasonic measurements the reader is referred to the accompanying paper [10].

## PROBLEM STATEMENT AND MODEL DESCRIPTION

We will concentrate our attention on titanium-based MMC considering SiC/Ti-15-3 composite as a modeling system. Using edge replica technique Johnson et al. [3] demonstrated that fatigue loading of  $[90]_8$  and  $[0/90]_{2s}$  SiC/Ti-15-3 laminates leads to fiber/matrix interface debonding in  $90^\circ$  lamina. Due to the presence of the carbon-rich coating in the SCS-6 fiber the strength of the bond between fiber and matrix is small. The main force which keeps fiber and matrix intact is the presence of residual stresses. An applied stress which exceeds the compressional radial residual stress causes fiber/matrix interface separation. Thus, it is expected that debonding will initiate in early stages of fatigue life after only a few cycles. Micrographic study reveals that for composites heat treated at  $815^\circ\text{C}$  the fatigue damage is dominated by fiber/matrix debonding in the  $90^\circ$  plies whose interfaces are perpendicular to the loading direction. The debonding of the circular fiber/matrix interface is partial (Fig. 1a): it first starts at the interface side perpendicular to the loading direction while interface parts oriented along the loading direction remain intact. As the damage progresses due to further fatigue cycling, the initial debond then extends over the entire interface.

The extent of debonding in [90] composite can be quantified by an angle  $\alpha$  (Fig. 1b). It defines the boundary between bonded and debonded parts of the fiber/matrix interface. When  $\alpha = 0^\circ$  there is no interfacial damage and  $\alpha = 90^\circ$  corresponds to complete fiber-matrix separation.

To apply the Generalized Method of Cells (GMC) for analysis of partially debonded fibers we build a representative volume element (RVE or repetitive cell) which allows one to predict changes in effective composite elastic constants as a function of  $\alpha$ . The constructed RVE is shown at Fig. 2a. It is based on discretization of the circular fiber. Subcells representing the fiber material are gray, while those of the matrix are white. Springs with zero stiffnesses ( $K_n = K_t = 0$ ) define the fiber/matrix boundary (dashed line) corresponding to the debonded region, while the boundary (solid line) in the bonded region is defined by springs of infinitely large stiffnesses ( $K_n = K_t = \infty$ ). Although stress concentration factors at the point of interfacial separation are not induced by this model, the softening influence of the fiber/matrix interface debond-

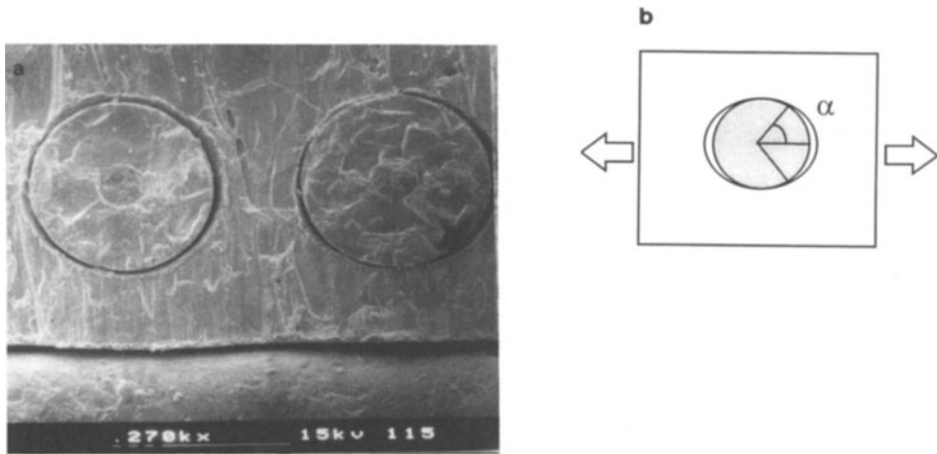


Figure 1. (a) Fiber/ matrix interface debonding in 90° ply of [0/90] SiC/Ti-15-3 composite after 50% of fatigue life; (b) Quantification of damage extent in [90] composite.

ing can be modeled by introducing interfacial subcells with changing properties or by defining spring boundary conditions.

In the case of cross-ply [0/90] composites the fatigue direction is parallel to the fibers in some plies (0° plies) and perpendicular in others (90° plies). It is reasonable to assume that in the first 50% of fatigue life the damage develops mainly in 90° plies in the form fiber/matrix interface debonding (Fig. 2b). Similar to the [90] composite the debonding in 90° ply can be characterized by the angle  $\alpha$  which separates debonded and bonded regions (Fig. 2b). In order to model damage in [0/90] composite we need to use a three dimensional RVE. It is built based on two dimensional RVE described above. Since no damage is assumed in the 0° ply, it is represented by a simple square fiber embedded in the matrix. The constructed RVE is shown in Fig. 2b. A circular fiber is taken for 90° ply and a square fiber for 0° ply. Debonding in 90° ply is modeled with springs of zero stiffnesses in a fashion similar to the [90] laminate.

The models described allow one to continuously monitor the reduction in effective composite moduli with damage evolution. This is done by changing  $\alpha$  and utilizing GMC with the above-described RVEs for calculation of composite moduli.

#### COMPARISON OF EFFECTIVE COMPOSITE MODULI DETERMINATION USING GMC, FEM and GSCM

GMC calculations of effective composite moduli are compared with finite element results for different fiber packings. We also compare GMC and Generalized Self Consistent Method (GSCM) predictions of the transverse shear modulus for 2-phase (fiber/matrix) and 3-phase (fiber/interphase/matrix) composite systems.

GMC has the capability of studying the effect of different fiber packings by building the appropriate representative volume element (RVE). The three most typical packing systems are square, diagonal and triangular. To compare the GMC predictions of effective composite moduli with FEM we use, as an example, Boron/Aluminum unidirectional composite. The constituent properties and the results of the FEM analysis are taken from Ref. [11]. The composite axial and transverse Young's moduli ( $E_a$ ,  $E_t$ ), Poisson's ratio ( $\nu_a$ ) and transverse shear modulus ( $G_t$ ) are calculated using GMC with

different fiber packings and are compared with the results for the same packings using FEM in Table 1. The best agreement is obtained for triangular fiber packing. As one can see GMC provides the same capabilities as FEM in studying different fiber arrangements but computationally it is more effective due to its analytical nature.

Also we compare GMC with the Generalized Self Consistent Model [12]. This is done for SiC/Ti composite without and with interphasial layer. All phases are assumed to be isotropic. The constituent properties are: fiber Young's modulus,  $E_f = 351$  MPa, fiber shear modulus,  $G_f = 148$  MPa, matrix Young's modulus,  $E_m = 99$  MPa and matrix shear modulus,  $G_m = 36.5$  MPa. The composite transverse shear modulus  $G_t$  is calculated as a function of fiber volume fraction and is shown in Fig. 3a. Calculations using GMC with square and triangular fiber packing are represented by squares and triangles respectively, the GSCM result is shown by the solid line. One can see that the estimates using GMC with triangular packing and GSCM agree well. Also calculations were made for the same SiC/Ti composite but now in addition con-

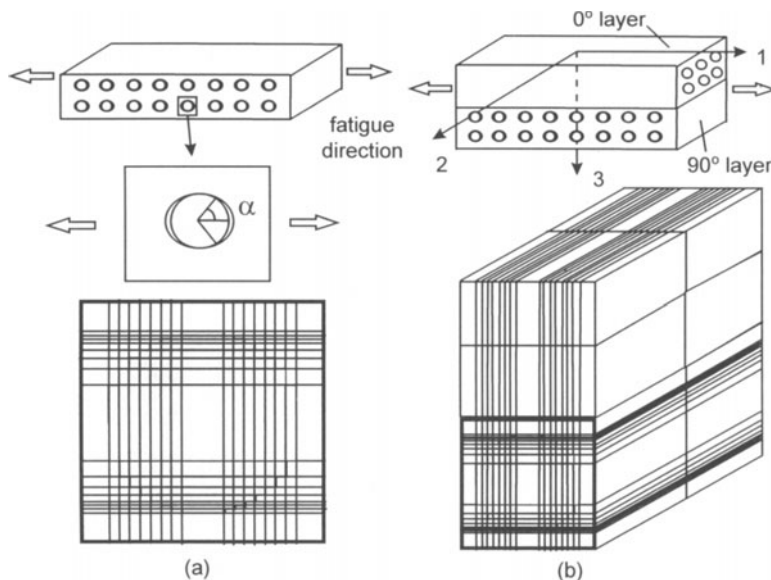


Figure 2. Fatigue damage modeling in (a) [90] and (b) [0/90] laminates.

sidering an interphasial layer. The thickness of the layer was taken to be 4.4% of the fiber radius. The Young's modulus of the interphasial layer was varied from  $0.05E_m$  to  $2E_m$ . The Poisson's ratio was kept unchanged and equal to the Poisson's ratio of the matrix,  $\nu_m = 0.356$ . The calculations of the transverse shear modulus for this system are shown in Fig. 3b. Again the results using GMC with triangular packing and GSCM agree well. The advantage of GMC versus GSCM for damage characterization is the ability to build an arbitrary RVE as shown above.

## APPLICATION TO EXPERIMENTAL DATA ANALYSIS

### Samples and fatigue testing

To illustrate the method's applicability we applied the model developed to quantify the damage in  $[0/90]_{2s}$  SiC/Ti-15V-3Cr-3Al-3Sn (SCS-6/Ti-15-3) metal matrix composites. The composite has an 8-ply symmetry layup made by hot isostatic pressing

Table 1. Predictions of effective moduli for Boron/Al composite using GMC and FEM. Fiber volume fraction is 46%.

Composite modulus	square pack		triangular pack		diagonal pack	
	GMC	FEM	GMC	FEM	GMC	FEM
$E_a$ , GPa	226	228	226	228	226	227
$E_t$ , GPa	146	153	134	138	121	134
$\nu_a$	0.265	0.266	0.264	0.262	0.270	0.262
$G_t$ , GPa	42.5	60	50.6	51	42.5	48

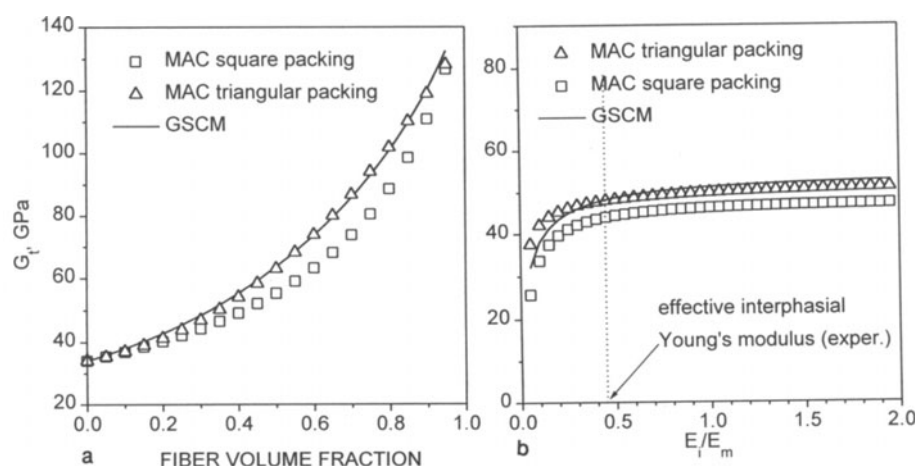


Figure 3. Predictions of the transverse shear modulus for (a) two-phase (fiber/matrix) and (b) three-phase (fiber/interphase/matrix) SiC/Ti composite using GMC and GSCM.

of a foil/fiber/foil layout. The matrix is metastable  $\beta$  titanium alloy Ti-15V-3Cr-3Al-3Sn (Ti-15-3, weight ratio) and the SiC fiber is SCS-6 by Textron. The fiber volume fraction of the composite is 35% and the composite density is 4.18 g/cm<sup>3</sup>.

Samples were heat treated for different exposure times (10 and 100 hours) at temperature 815°C. The heat treated samples were first fatigued to failure under different stress ranges to obtain their S/N curves. Based on the S/N curves, two stress-controlled fatigue tests ( $\Delta\sigma$  equals 50 or 70% of the ultimate strength,  $R = \sigma_{min}/\sigma_{max} = 0.1$ ) were selected for ultrasonic damage assessment using samples with different heat exposure times. It has been shown in several studies [3, 4] that the threshold stress level for this composite system, below which no fatigue damage will occur, is about 500 MPa. This level is about 40 percent of the ultimate strength, which is only slightly lower than the selected stress ranges. The fatigue cycling frequency is 10 Hz. Ultrasonic bulk wave velocity and attenuation measurements were performed on samples prior to fatigue as well as at different stages of fatigue (with step size 0.1 of the fatigue life).

#### Ultrasonic velocity measurements and determination of effective composite moduli

A self-reference bulk wave method [13] was used to measure the ultrasonic phase veloc-

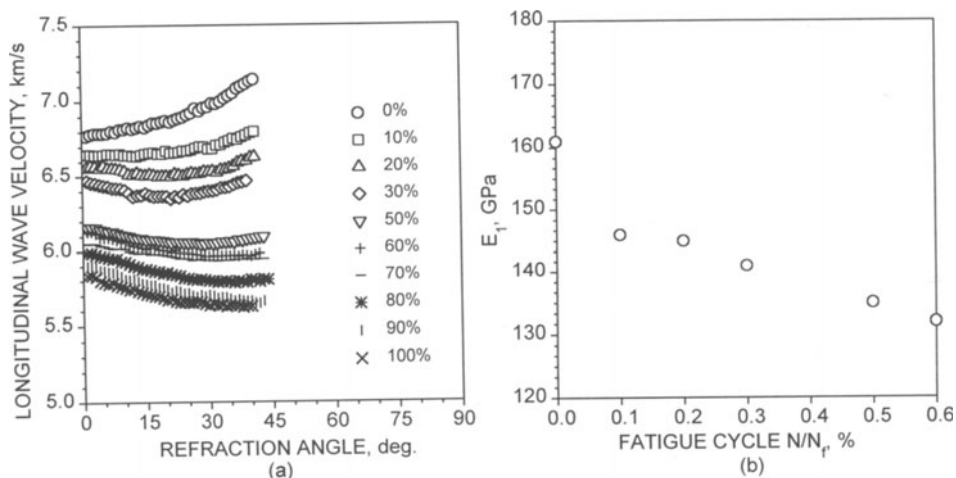


Figure 4. (a) The measured wave velocities versus refraction angle at different stages of fatigue damage; (b) The composite Young's modulus in the loading direction versus number of fatigue cycles.

ities in the composite samples. The measurements were made in a computer-controlled goniometer using a 5 MHz immersion transducer. Angular resolution and repeatability were better than 0.01 degree. The water temperature inside the goniometer was stabilized at  $29.8 \pm 0.01^\circ \text{C}$ .

Ultrasonic wave velocities were measured in several incident planes (parallel or normal to the loading direction). The coordinate system is selected so that axis 1 is along the loading direction (the fiber direction in the  $0^\circ$  plies) and axis 2 is along the fiber direction in the  $90^\circ$  plies as shown in Fig. 2b.

In each incident plane the time delay was measured as a function of incident angle and used to calculate wave propagation velocities at different refraction angles. The ultrasonic wave velocities were found to decrease as the number of fatigue cycles increases. Fig. 4a shows the quasi-longitudinal wave velocities versus refraction angle (propagation direction) in the 1-3 plane (parallel to the loading) for a composite heat treated for 100 hours before fatigue and at different stages of fatigue life. In addition to the reduction of the velocity, the angular dependence of the velocity is changed due to the development of fatigue damage.

The damage described above is consistent with the ultrasonic results in the 1-3 plane. When ultrasonic waves propagate parallel (at normal incidence) to the crack-like fiber/matrix debonds, the velocities are less affected by the damage. On the other hand, when the ultrasonic waves propagate nearly perpendicular (at oblique incidence) to the debonds, the velocities are greatly reduced by the microdamage. Thus the ultrasonic velocities for samples with and without fatigue damage (fiber debonding) have different angular dependence.

Since the ultrasonic wavelength used experimentally is approximately five times greater than the lamina thickness (0.21 mm), one can use the measured velocity data to determine the effective moduli of the cross-ply composite. In this case, the calculated composite moduli represent ultrasonically averaged composite properties with respect to a specific layup, considering the composite as a homogeneous material. Also since wave dispersion is very small in this frequency range, the elastic constants deter-

Table 2. Damage predictions in 90° of [0/90] SiC/Ti-15-3 composite from ultrasonically measured effective composite moduli.

$N/N_f$	Experiment		Model damage prediction
	$E_1$ , GPa	$E_3$ , GPa	$\alpha$ , deg.
0	161	138	0
0.1	146	132	18.6
0.2	145	129	19.9
0.3	141	126	25.2
0.5	135	120	33.6
0.6	132	119	38.1

mined are close to the static limit ( $\omega \rightarrow 0$ ). To determine the composite moduli we use an inverse approach applying the nonlinear least-squares optimization technique [14].

#### Inverse determination of interfacial damage extent from experimental data

Now our goal is to relate the reduction in effective composite moduli to the quantitative damage parameter introduced in the previous section. Fiber/ matrix interface debonding in 90° ply affects mostly composite properties in the loading direction (1-direction at Fig. 2b) and to a less extent in the through-thickness direction (3-direction). Properties in the fiber direction of 90° ply (2-direction) are almost unaffected by debonding in this ply. Thus for the determination of the angle  $\alpha$  which characterizes the extent of debonding in 90° ply we choose Young's moduli in 1- and 3-directions,  $E_1$  and  $E_3$ . To find  $\alpha$  we solve the inversion problem by minimizing the difference between Young's moduli ( $E_1^{exp}$ ,  $E_3^{exp}$ ) determined from experimental velocity data and calculated using GMC ( $E_1^{calc}$ ,  $E_3^{calc}$ ):

$$\min_{\alpha \in [0, 90]} \frac{1}{2} [(E_1^{exp} - E_1^{calc})^2 + (E_3^{exp} - E_3^{calc})^2]. \quad (1)$$

The reduction in the composite Young's modulus ( $E_1$ ) as a function of the number of fatigue cycles  $N$  normalized by the number of fatigue cycles to failure  $N_f$  is shown at Fig. 4b. In the first 50% of fatigue life one can observe significant reduction in the moduli. We assume that at this stage the dominant damage mechanism is fiber/matrix interphase debonding and employ the inversion procedure (1) to determine the damage parameter  $\alpha$ . The inversion results are summarized in Table 2 for a sample heat treated for 100 hours and fatigued with  $\delta\sigma = 0.5\sigma_u$ . Significant debonding ( $\alpha = 18.6^\circ$ ) is predicted already at 10% of the fatigue life. This indicates that damage starts developing in early stages of fatigue life. At 60% of fatigue life  $\alpha$  reaches almost 40° which means that almost half of the fiber/matrix interface is separated. In the second 50% of fatigue life other damage mechanisms such as matrix cracking and fiber breakage start to play a major role and can no longer be ignored.

#### SUMMARY

A model has been developed to quantify fatigue damage evolution in metal matrix composites. A quantitative debonding area parameter is introduced which characterizes fiber/ matrix interface debonding in [90] unidirectional composites and in 90° plies of cross-ply composites. Micromechanical analysis has been performed to relate debonding area to effective composite moduli. It is based on Generalized Method of Cells (GMC) and is applied to perform debonding modeling. The method's applicability has been demonstrated in the example of [0/90]<sub>2s</sub> SCS-6/Ti-15-3 composite for which ultrasonic data were collected. It was found that fiber/matrix interface debond-

ing in 90° plies starts in early stages of fatigue life. At 50% of fatigue life approximately half of the fiber/matrix interface is separated. Thus the method has potential for prediction of remaining fatigue life.

## ACKNOWLEDGEMENTS

This work was sponsored by NASA Lewis Research Center under grant #NAS3-97030. Dr. George Y. Baaklini and Dr. H. Roth are the program monitors. The authors thank Dr. Steven M. Arnold of NASA Lewis Research Center for providing Micromechanical Analysis Code (MAC) and useful discussion of the code capabilities and utilization.

## REFERENCES

1. S. Mall and B. D. Portner, ASME AMD 118, 239 (1991).
2. T. P. Gabb, J. Gayda, B. A. Lerch and G. R. Halford, Scripta Metall. et Mater. 25, 2879 (1991).
3. W. S. Johnson, S. J. Lubowinski and A. L. Highsmith, in *Thermal and Mechanical Behavior of Metal Matrix and Ceramic Matrix Composites* ASTM, 193 (1990).
4. R. A. Naik and W. S. Johnson, NASA TM101688 (1990).
5. S. I. Rokhlin, Y. C. Chu and W. Huang, Mechanics of Materials 21, 251 (1995).
6. S. Baste and R. El Bouazzaoui, J. Compos. Mat. 30, 282 (1996).
7. J. Aboudi, *Mechanics of Composite Materials. A Unified Micromechanical Approach* (Elsevier, Netherlands, 1991).
8. M. Paley and J. Aboudi, Mechanics of Materials 14, 127 (1992).
9. T. E. Wilt and S. M. Arnold, NASA TM107290 (1996).
10. S. I. Rokhlin, M. Ganor and A. D. Degtyar, in Review of Progress in Quantitative NDE, Vol. 17, D. O. Thompson and D. E. Chimenti, Eds. (Plenum Press, N.Y., 1998).
11. J. R. Brockenbrough, S. Suresh and H. A. Wienecke, Acta Metall. Mater. 39, 735 (1991).
12. W. Huang and S. I. Rokhlin, Mechanics of Materials 22, 219 (1996).
13. Y. C. Chu and S. I. Rokhlin, J. Acoust. Soc. Am. 92, 920 (1992).
14. S. I. Rokhlin and W. Wang, J. Acoust. Soc. Am. 91, 3303 (1992).